

# User-adaptive Eyelid Aperture Estimation for Blink Detection in Driver Monitoring Systems

Juan Diego Ortega<sup>1,2</sup>, Marcos Nieto<sup>1</sup>, Luis Salgado<sup>3</sup> and Oihana Otaegui<sup>1</sup>

<sup>1</sup>*Vicomtech Foundation, Basque Research and Technology Alliance (BRTA), Donostia-San Sebastián, Spain*

<sup>2</sup>*Departamento de Señales, Sistemas y Radiocomunicaciones, ETS Ingenieros de Telecomunicación, Universidad Politécnica de Madrid (UPM), Madrid, Spain*

<sup>3</sup>*Grupo de Tratamiento de Imágenes, Information Processing and Telecommunications Center (IPTC) and ETS Ingenieros de Telecomunicación, Universidad Politécnica de Madrid (UPM), Madrid, Spain*

**Keywords:** Eyelid Aperture, Blink Detection, Driver Monitoring, Computer Vision, ADAS.

**Abstract:** This paper presents a new method for eyelid aperture estimation, suitable to be used in Driver Monitoring Systems (DMS) to measure blink patterns such as microsleeps and any other metric that assess the fatigue level of the driver. The method has been designed to work real-time and in continuous operation, by introducing a novel online Exponential Weighted Moving Average (EWMA)-based Bayesian estimation process, which ensures dynamic adaptability to drivers with different physiognomy features, and also to changes due to physiological states (e.g. drowsiness). Our method has been implemented in the framework of a DMS, to take advantage of existing facial landmark detection and tracking mechanisms, and to provide real-time functionality for driving platforms (such as the NVIDIA Drive PX 2). The method is evaluated against a large labelled dataset, and compared to baseline and previous existing methods, showing an excellent balance between adaptability, performance, and robustness.

## 1 INTRODUCTION

Drowsy driving is an important cause of road accidents. Studies have shown that up to 6% of all motor vehicle crashes were related to drivers whose performance was impaired by fatigue. More dramatically, in the EU, 20% of truck-involved fatal crashes were related with fatigued drivers (SafetyNet, 2009). Therefore, the automobile industry is pushing forward the development of fully autonomous vehicles whose aim is to reduce crashes due to driver errors, eventually achieving the desired zero-accident road scenario (European Commission, 2011).

While Level-5 of driving automation is the ultimate goal, Levels-1, 2, and 3 still consider the active presence of a human driver in the car (SAE International, 2018). Therefore, modern Advanced Driver Assistance Systems (ADAS) developers have increasingly consider to include Driver Monitoring Systems (DMS) to achieve a holistic understanding of the

scene. DMS are crucial to analyse the driver status for an enhanced and safer mode transfer between autonomous and manual operation (Cabral et al., 2016).

Over the past decade, works on DMS have proposed methods to determine fatigue and distraction attending to the type of inputs from the driver. Traditionally, DMSs had relied on vehicular features to determine driver inattention (e.g. steering wheel angle, pedal action, lane deviation, etc.) (Boyle et al., 2008). However, when using highly autonomous vehicles, these features will not be available as the driver is not manipulating the vehicle, making it difficult to continuously monitor the driver state.

Other works studied biological features of the driver (e.g. heart, brain, skin signals) (Borghini et al., 2014) using devices attached to the driver. These methods require expensive intrusive sensors which make them unfeasible for real applications in vehicles.

Drivers also exhibit certain observable behaviour such as eyelid and head movements that correlate significantly with distraction and drowsiness. Besides, the advances in computer vision research have made it possible to robustly extract observable features from

<sup>a</sup>  <https://orcid.org/0000-0001-5539-106X>

<sup>b</sup>  <https://orcid.org/0000-0001-9879-0992>

<sup>c</sup>  <https://orcid.org/0000-0002-5364-9837>

<sup>d</sup>  <https://orcid.org/0000-0001-6069-8787>

the driver face with unobtrusive sensors (Sikander and Anwar, 2019).

One of the most reliable physiological indicator for determining the driver status is the eyelid aperture level (Danisman et al., 2010). In addition, the use of ocular dynamics are proven to be the most robust and meaningful method for drivers' fatigue and distraction assessment (Sikander and Anwar, 2019). The eyelid aperture level is the basic measure to obtain more complex and discriminative indicators such as blink duration, blink frequency or PERCLOS. The last being widely used in the literature (Kaplan et al., 2015) to determine the fatigue state of the driver.

Scientific works on blink detection could be categorised in three main groups: (i) appearance-based methods, (ii) motion-based methods and (iii) shape-based methods. Appearance based methods determine the eye state by either using templates for open and closed eyes (González-Ortega et al., 2013) or trained classifiers using machine learning (Han et al., 2016; Mandal et al., 2017). In (Danisman et al., 2010) visual changes in eye states are detected using the horizontal symmetry feature of eyes, while (Daniluk et al., 2014) computes horizontal and vertical filters to detect eyelids. Moreover, motion-based methods typically require to first detect the face and eye regions within the image by means of statistical classifiers. Then, motion in the eye area is estimated from optical flow (Fogelton and Benesova, 2016; Drutarovsky and Fogelton, 2015). Finally, a decision is made whether the eyes are or are not covered by the eyelids.

A major drawback of the previous two groups is that they determine a discrete number of eye states (i.e. close/open or close/transition/open), instead of measuring a continuous value of aperture, which can be used to extract more complex information about blinking patterns, such as the closing and opening duration of blinks.

Shape-based method, on the other hand, obtain the contour of the eyelid borders and compute an indicator of the degree of eye aperture. Then, thresholds for the eyelid aperture (Schmidt et al., 2018), classification algorithms (Soukupová and Cech, 2016) or rule-based methods (Baccour et al., 2019) are used to detect blinks.

The signals to compute the contour of the palpebral fissure can be obtained by image processing algorithms such as the adjustment of an Active Shape Model (ASM) (Yang et al., 2012) or a Regression Landmark Model (Gou et al., 2017). These methods are suitable and practical in the context of real DMS solutions where face landmark detection is required for several functions, such as blink analysis, head pose estimation, or gaze estimation refinement

(Fridman et al., 2016; Goenexea et al., 2018).

Different approaches have been used to compute the eyelid aperture measurement. For instance, (Fuhl et al., 2017) approximate the upper and bottom eyelids contours by fitting two intersected parabolic functions, one per eyelid border. The eyelid aperture is estimated by using the distance from the upper and lower eyelid curves.

In (Wang et al., 2009) an 8-point eye deformable model is proposed. The eyelid aperture level degree is obtained by computing the ratio of the maximum vertical distance and the intra-ocular distance (IOD) for each eye. Eye blink detection is determined by applying an heuristic threshold determined by a set of evaluation face data. Similarly, in (Yang et al., 2012), a face tracker based on ASM is computed to obtain a first position of eye landmarks. Then the eye contour is refined by fitting a deformable template of two intersected parabolic sections to a distance map based on the distance of each pixel to the distribution of the skin colours. The final eye closure score is evaluated from the converged eye shape.

Blink detectors face three main challenges. First, it is difficult to reliably distinguish between eye blink events and gaze-related eyelid closure, specially glances to the dashboard (Friedrichs and Yang, 2010). Second, the inter-individual differences in palpebral fissure of the drivers make it difficult to detect blinks when fixed thresholds are used for all individuals (Schmidt et al., 2018). Third, driver arousal state, such as drowsiness, has a strong impact in the eyelid aperture signal (Ebrahim et al., 2013) making it necessary to introduce an adaptive algorithm to overcome the intra-individual variability of eyelid aperture.

Past works have included some strategies to overcome these challenges. For instance, in (Nopsuwanchai et al., 2008) they apply an statistical ASM to fit a set of 20 points corresponding to the outline of upper and lower eyelids. The eyelid aperture level is defined as the ratio between the maximum vertical distance (height,  $H$ ) and the maximum horizontal distance (width,  $W$ ) of the eye. To cope the inter-individual variability, the eyelid aperture measurement is normalised. The eyelid aperture measurement at frame  $t$ ,  $A_t$ , is normalised to  $A_{n,t}$  by:

$$A_{n,t} = \frac{A_t - A_{c,t}}{A_{o,t} - A_{c,t}} \quad (1)$$

where  $A_{o,t}$  and  $A_{c,t}$  is the average value of open-eye aperture and closed-eye apertures, respectively. The maximum opening and closing aperture level is computed by averaging a ground truth data for 'standard' blinks for each individual driver. Therefore, these

methods do not automatically compute the normalisation parameters ( $A_{o,t}$  and  $A_{c,t}$ ).

The method proposed in (Sukno et al., 2009) is based on ASM with Invariant Optimal Features (IOF-ASM). The quantification of eyelid aperture is determined by the average of vertical distance of eye landmarks. Then, the aperture value is normalised by statistics estimated by observing a longer sequence. The main drawback of these methods is that the user-dependant signals used to normalise the eyelid aperture metrics are computed taking a set of data before-hand, which make these methods not suitable for online applications.

In (Soukupová and Cech, 2016) facial landmark detectors are used to localise the eyes and eyelid contours combined with a classifier that is trained to recognise eye blinks. The eye aspect ratio computed from the landmarks is used as an estimate of the degree of eyelid openness. An SVM classifier of fixed temporal windows is trained to detect eye blinks. However, using a fixed temporal window for all subjects may produce mistakes in blink detection since different individuals with different attentiveness states could show different blink patterns. Moreover, in (Gou et al., 2017) a joint cascaded framework for simultaneously detect eye landmarks and eye openness probability is proposed. The method rely on the availability of a large labelled dataset to achieve good results which could limit the applicability of the method if such database is not available.

In some recent methods such as (Baccour et al., 2019), a rules-based method is proposed. The steps to define blink features is obtained by analysing the properties of blinks. The method uses a filtered signal of the eye closure and its derivative to calculate the start and end of blinks. The method defines standard steps for regular blinks and special cases are considered. Nevertheless, the computation of some of the design thresholds are done taking a temporal windows of several minutes which prevents it to be used in continuous driving monitoring.

To overcome the different challenges of eye blink detection, in this paper we present a method for online eyelid aperture normalisation, based on robust facial landmark points, which is invariant to image scale and adapts to driver physiological features. A learning process based on eye state-balanced cost function is applied to obtain the optimal model parameters using a training set composed of several subjects with different attentiveness states. Our method can be categorised as a shape-based eyelid detection method, which overcomes the rigidity inherent to previous works which do not adapt online to each individual, or to different physiological states.

Our method improves other blink detection approaches as it outputs a driver-adaptive eyelid aperture signal, meaning that, for two individuals with different eye physiognomy, the palpebral fissure amplitude will be always retrieve an equivalent eyelid aperture value between 0 and 1, being 0 a totally closed eye and 1 when the eye is completely open.

We have implemented the proposed method in the context of a DMS framework, which works online in different platforms and is compatible with existing third-party libraries. Experimental results of our proposed method support our claims, including a comparison with other baseline methods and implementation on different hardware setups: our method shows improved accuracy in a binary classification of eye states, making it suitable for integration in complex real-time DMS pipelines.

The paper is organised as follows. Section 2 details the proposed method for eyelid aperture normalisation. Section 3 describes the method to select the parameters of our algorithm. Section 4 Describes the platforms in which our method was integrated. Section 5 reviews evaluation of our method based on a defined cost function and accuracy of the classification of opened and closed (blink) states.

## 2 EYELID APERTURE ESTIMATION METHOD

It is well known that the shape of human eye varies between individuals. Different factors such as ethnicity, age and gender can make the individuals to have this variability. Then, the method that characterises the palpebral fissure should learn from observations what is the current degree of eye aperture based on the maximum and minimum eyelid aperture levels for the opened and closed eye states, respectively. This dynamic information allows the method to normalise the eyelid aperture level to be user-agnostic.

Note that we distinguish between eyelid amplitude and normalised eyelid aperture. In this work the eyelid amplitude is referred as a value obtained from ratios of eye dimensions; while the normalised eyelid aperture, or simply the eyelid aperture is the degree of openness of an eye. It is described as a value between 0 (closed-eye) to 1 (open-eye).

The applications of eyelid aperture detection are many. For instance, to detect eye blinks and measure their duration, amplitude, frequency or PERCLOS. DMS applications can use this valuable information to learn and predict drowsiness and fatigue state of drivers.

## 2.1 Definition of Eyelid Amplitude

We choose to use facial landmarks models to extract eye dimensions. There are robust real-time facial landmark detectors available in the literature (Asthana et al., 2014; Kazemi and Sullivan, 2014) and as open-source libraries: DLib ERT (King, 2009) or OpenFace (Baltrusaitis et al., 2016)) that allows to obtain the eye dimensions. Besides, the information of the facial landmarks could be used by other driver monitoring methods such as head pose estimation and gaze estimation, reducing the computational overhead of algorithms in complex systems, obtaining real-time integrated DMS applications.

Face alignment methods compute the eye shape as a connected set of feature points. Therefore, a measure of the eyelid amplitude is necessary to obtain the final eye aperture level. In the literature different methods for measuring the eyelid amplitude from landmarks are proposed.

In (Sukno et al., 2009) the amplitude is measured as the mean distance between vertically corresponding landmarks. Similarly, in (García et al., 2012) the eye amplitude is defined as the height between eyelids. However, these methods will not tolerate changes of scale. In contrast, other authors (Soukupová and Cech, 2016; Mandal et al., 2017) suggest to use scale-independent metrics where the measure involves using a ratio of a vertical and horizontal distance.

Moreover, in (Baccour et al., 2019), the eye closure is obtained from the ratio between the vertical distance between eyelids and a fixed diameter of the iris. However, to obtain real dimensions of the eye this method should need to have a calibrated camera which could not be possible in all DMSs.

In our approach the eye amplitude  $A_t$  is set as the eye aspect ratio (EAR) between height and width. We take the eye contour landmarks provided by our facial landmark model and compute the eye aspect ratio using the maximum height  $H_t$  and width  $W_t$  of the contour of the facial points as shown in Figure 1.

The eye usually has an rectangular shape (i.e. the width is larger than height); therefore, to obtain values closer to one when the EAR is maximum, we propose to use the double of the EAR as the value of eye amplitude to be normalised by our method (eq. 2).

$$A_t = \min \left( 1, \frac{2H_t}{W_t} \right) \quad (2)$$

The eye amplitude  $A_t$  saturates to 1 for eyes whose height is half the width, which is something that may occur for very round eyes. Depending on the physiological state and the facial physiognomy of indi-

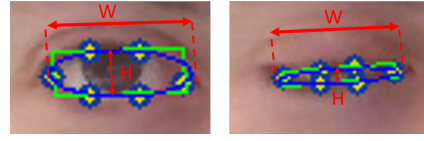


Figure 1: Eye landmark fitting and estimation of the height ( $H$ ) and width ( $W$ ) of the eye.

viduals, the nominal amplitude level for opened and closed eye may be different between each others. Figure 2 illustrates this difference: we can observe that different individuals have different maximum and minimum  $A$  values.

## 2.2 Normalised Aperture Estimation

The eyelid amplitude  $A_t$  value (eq. 2) should be normalised to obtain an aperture level, which is robust to changes of subject facial characteristics. The computation of the normalised eyelid aperture  $A_{n,t}$ , for each time frame  $t$  is achieved using an online probabilistic approach, which computes the posterior probability of the event where eye is open  $E_{o,t}$  and closed  $E_{c,t}$ , such as  $A_{n,t} = P(E_{o,t}|A_t)$ .

Using the Bayesian formulation we have the following expressions:

$$P(E_{o,t}|A_t) = \frac{p(A_t|E_{o,t})P(E_{o,t})}{P(A_t)}; \quad (3)$$

$$P(E_{c,t}|A_t) = \frac{p(A_t|E_{c,t})P(E_{c,t})}{P(A_t)} \quad (4)$$

where  $p(A_t|E_{o,t})$  and  $p(A_t|E_{c,t})$  are the probability density functions that represent the likelihood of observing the eye in open and closed states, respectively.  $P(E_{o,t})$  and  $P(E_{c,t})$  are the a priori probability of each event, and  $P(A_t)$  is the evidence, a normalisation factor to ensure  $\sum_{s \in \{o,c\}} P(E_{s,t}|A_t) = 1$ , which is computed as  $P(A_t) = \sum_{s \in \{o,c\}} p(A_t|E_{s,t})P(E_{s,t})$ .

The likelihood models are derived from two balanced distributions, truncated at their extremes:

$$p(A_t|E_{o,t}) = \omega_g(A_t)g(A_t|A_{o,t-1}; \text{Var}(A_{o,t-1})) + \omega_u(A_t)u(A_t|A_{o,t-1}, 1) \quad (5)$$

where  $g(A_t|A_{o,t-1}; \text{Var}(A_{o,t-1}))$  is the normal distribution with mean equal to  $A_{o,t-1}$  and variance equal to the variance of  $A_{o,t-1}$ ; and  $u(A_t|A_{o,t-1}, 1)$  is a uniform distribution in the interval  $(A_{o,t-1}, 1)$ , scaled to  $g(A_{o,t-1})$ . The factors  $\omega_g$  and  $\omega_u$  are step functions which determine the application of functions  $g$  and  $u$ , respectively:  $\omega_g(A_t) = 1$  for  $A_t \leq A_{o,t-1}$  and  $\omega_u(A_t) = 1$  for  $A_t > A_{o,t-1}$ . The likelihood of  $A_t$  of event  $E_{c,t}$ ,  $p(A_t|E_{c,t})$  can be expressed analogously.

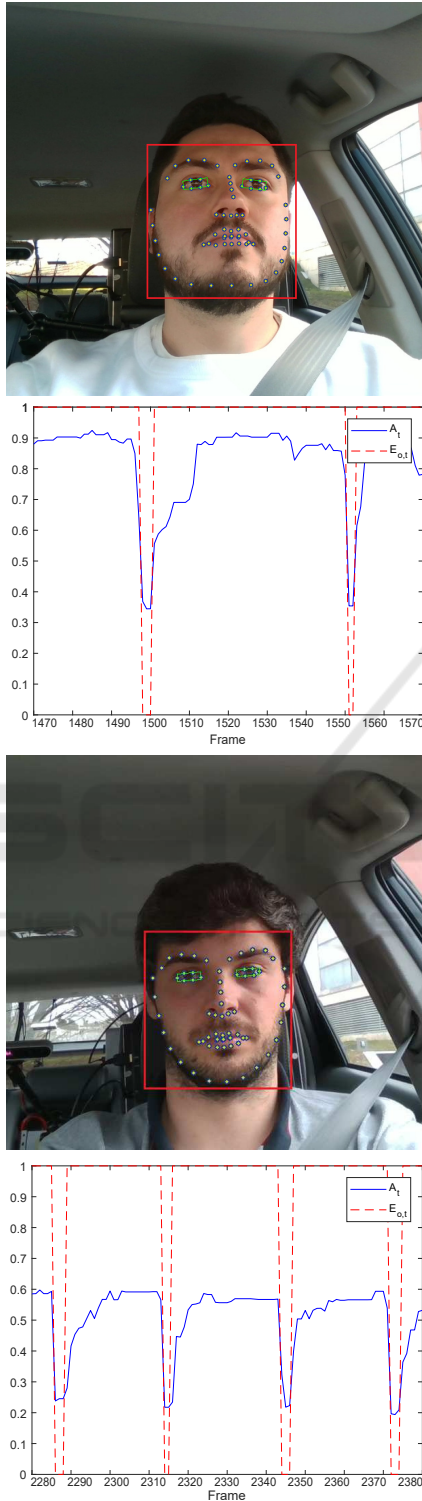


Figure 2: Differences in eyelid amplitude for two different individuals blinking normally. The graphs below each user's frame show the corresponding amplitude  $A_t$  computed as in eq. 2.

Updating the values of  $A_{o,t}$  and  $A_{c,t}$  makes the entire process recursive. For that purpose, we propose to estimate these values as Exponential Weighted Moving Averages (EWMA) (Friedrichs and Yang, 2010) whose learning factors are updated at each frame according to a function which determines the local variability of the signal in a temporal window:

$$A_{o,t} = \omega_o A_{o,t-1} + (1 - \omega_o)A_t \quad (6)$$

$$A_{c,t} = \omega_c A_{c,t-1} + (1 - \omega_c)A_t \quad (7)$$

The learning factors,  $\omega_o$  and  $\omega_c$ , are not static, but defined as dynamic values to increase the impact of a new measurement  $A_t$  according to its distance to  $A_{o,t-1}$  and  $A_{c,t-1}$ , i.e. when  $A_t$  is very close to  $A_{o,t-1}$  then its impact on  $A_{o,t}$  update is higher (by decreasing  $\omega_o$ ).

Therefore, we build signal  $A_{s,t}$ , which is the EWMA of measurement  $A_t$ .

$$A_{s,t} = \alpha A_{s,t-1} + (1 - \alpha)A_t \quad (8)$$

where  $\alpha$  is the averaging factor of  $A_{s,t}$ .

Under the hypothesis that the time eyes are open is higher than the time eyes are closed, then  $A_{s,t}$  is always closer to  $A_{o,t}$  than to  $A_{c,t}$ . Therefore, we can use  $A_{s,t}$  to define the value of  $\omega_o$ . A way to implement this idea, and also provide a mechanism to define  $\omega_c$  is to create a sigmoid function (which returns a value between 0 and 1) on the difference between  $A_t$  and  $A_{s,t-1}$  (higher values of this sigmoid corresponds to situations the eye is more likely open, and lower values correspond to closed eye measurements). The sigmoid function is defined as:

$$\Phi(A_{s,t} - A_t) = \frac{1}{1 + e^{-a(A_{s,t} - A_t - c)}} \quad (9)$$

where variables  $a$  and  $c$  can be selected to make the sigmoid function be centred at  $c = (A_{o,t} - A_{c,t})/2$  (i.e. the expected mid-way between the eye amplitudes at open and closed states), and to reach a significant value at the maximum possible difference, e.g.  $\Phi(A_{o,t} - A_{c,t}) = 0.95$  (note the sigmoid function asymptotically approaches to 1 but without never reaching it):

$$a = -\frac{\log\left(\frac{1}{\Phi(A_{o,t} - A_{c,t})} - 1\right)}{A_{o,t} - A_{c,t} - c} \quad (10)$$

Figure 3 details the evolution of the involved functions in the computation of the normalised aperture. Note in second row, the values of the sigmoid range from 0 to 1, following the variability of  $A_t$ . In practice, this variability is counterproductive for an

EWMA learning factor (i.e. it makes the EWMA not smooth). Therefore, the learning factor update equation needs to be regularised as follows:

$$\omega_o = \beta + (1 - \beta)\Phi(A_{s,t} - A_t) \quad (11)$$

$$\omega_c = \beta + (1 - \beta)(1 - \Phi(A_{s,t} - A_t)) \quad (12)$$

These learning factors leads to smoother evolution of  $A_{o,t}$  and  $A_{c,t}$ . Parameter  $\beta$  is a user-defined parameter that balances the impact of  $\Phi$ .

In addition, Figure 4 illustrates the values of the computed amplitudes on a sample 500 frames sequence. As we can observe, the EWMA is slowly learning the average of  $A_t$ , while  $A_{o,t}$  and  $A_{c,t}$  adapt to the observed open and closed-eye amplitudes (a full discussion on the learning rates for each signal is provided in section 3). For this example the following constants were used:  $\alpha = 0.999$  and  $\beta = 0.99$ . It is possible to see that  $\Phi$  determines how likely the measurement belongs to the open and closed states, and the learning factors  $\omega_o$  and  $\omega_c$  are updated according to  $\Phi$ . In other words, the average closed-eye amplitude  $A_{c,t}$  is updated with significant weight, assigned to the current measurement  $A_t$  proportionally to  $\omega_c$ , which corresponds to the situations where the eye is likely closed.

### 3 PARAMETER LEARNING

#### 3.1 Manual Parameter Selection

The two design parameters of the our method are  $\alpha$  and  $\beta$ . On the one hand,  $\alpha$  determines how fast the EWMA  $A_{s,t}$  learns from observed measurements, while  $\beta$  determines the amount of impact function  $\Phi$  can have on the estimation of the amplitude values for open and closed-eye states,  $A_{o,t}$  and  $A_{c,t}$ .

It is noteworthy to mention that the learning parameters of the EWMA expressions are inversely proportional to the learning speed of the function, i.e. values closer to 1 (e.g. 0.9999) express slower learning rates than smaller values. Therefore, their selection is critical to get the expected behaviour.

We can select values for this parameters by defining what is the expected learning period for the estimated magnitudes. For that purpose, we can rewrite the EWMA equation (eq. 8) as time series:

$$A_{s,t} = \alpha^t A_{s,0} + (1 - \alpha) \sum_{i=1}^t \alpha^{t-i} A_i \quad (13)$$

From this expression, and considering an extreme case where EWMA is initialised to 1.0, and then all

subsequent measurements are 0.0, we can define the equivalent time period to decrease  $x\%$  as:

$$T_x = \frac{\log(1-x)}{\log(\alpha)} \quad (14)$$

and reversely,

$$\alpha = \exp\left(\frac{\log(1-x)}{T_x}\right) \quad (15)$$

This equation can be used to obtain a guess on the required value of the learning parameter  $\alpha$  for a certain period, e.g.  $T_{95}$ . For instance,  $\alpha$  should be at least 0.999 to get a period of about 1000 frames, which corresponds to 40 seconds at 25 fps, because the average value of the eyelid amplitude  $A_{s,t}$  should not change faster than that (physiologically, average eyelid amplitude changes slowly due to fatigue factors (Sikander and Anwar, 2019)). Similar procedure can be done over eq. 11 to obtain an estimation of  $\beta$ . Therefore,  $\beta$  should be around 0.99 to get faster adaptation ( $T_{95}(0.99) = 50$ ) to the expected value of open and closed-eye amplitudes,  $A_{o,t}$ ,  $A_{c,t}$ , which can dynamically change due to face gestures, gaze patterns (e.g. looking to the dashboard), etc.

#### 3.2 Parameter Training

However, to improve the adaptability of the method to the data of each user, the selection of the values for  $\alpha$  and  $\beta$  should be done automatically. We propose to defining a cost function and using a training set which covers a variety of subjects and blinking situations.

Let us consider  $E_{o,t}$ , a binary signal whose value is 1 and 0 when the eye is in open and closed, respectively, and  $O$  the set of time indexes for which  $A_{n,t} > 0.5$  (i.e. the method is classifying the eye as open) and  $C$  the set of tie indexes for which  $A_{n,t} \leq 0.5$  (i.e. classified as closed). Then, we define a cost function which penalises the errors between the predicted normalised eyelid aperture and the ground truth labels. The objective is to obtain the values for  $\alpha$  and  $\beta$  that minimize the following cost function:

$$J = \frac{1}{|O|} \sum_{t \in O} \rho(A_{n,t}, E_{o,t}) + \frac{1}{|C|} \sum_{t \in C} \rho(A_{n,t}, E_{o,t}) + \frac{1}{|O \cup C|} \sum_t \gamma(A_{n,t}, E_{o,t}, \tau) \quad (16)$$

where  $|O|$  and  $|C|$  are the cardinalities of sets  $O$  and  $C$  respectively, and  $\rho()$  is a M-estimator of the squared

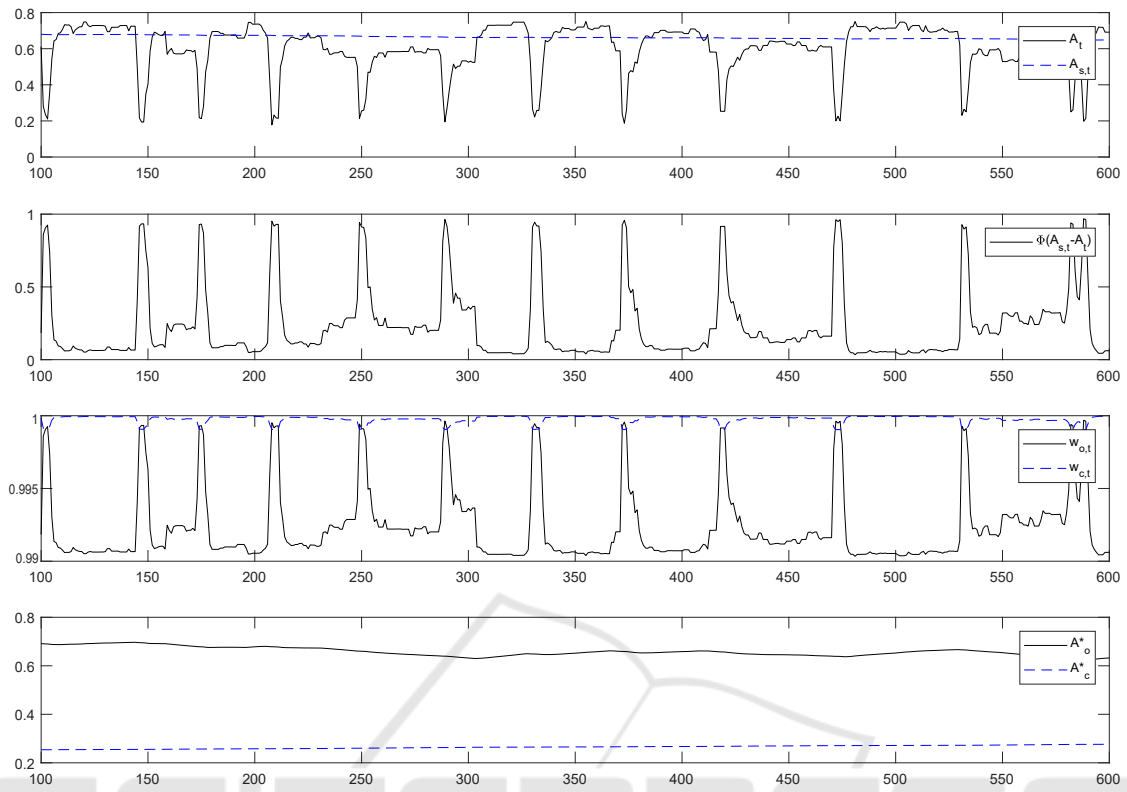


Figure 3: Values of the different parameters involved in the computation of the normalised aperture for a sample sequence.

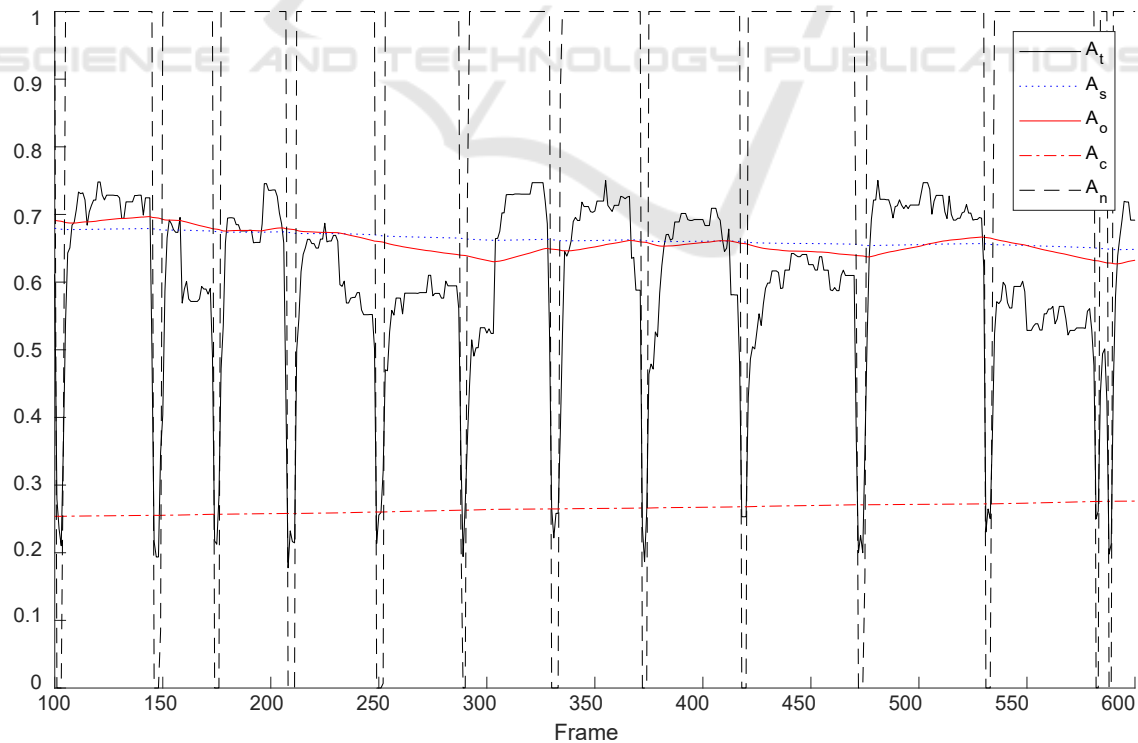


Figure 4: Sample values of eyelid closure  $A_t$ , EWMA  $A_{s,t}$ , open and closed-eye estimated amplitudes  $A_{o,t}$  and  $A_{c,t}$ , and normalised aperture  $A_{n,t}$ .

difference:

$$\rho(A_{n,t}, E_{o,t}) = \begin{cases} (A_{n,t} - E_{o,t})^2 & , if |A_{n,t} - E_{o,t}| < \varepsilon \\ \varepsilon^2 & , otherwise \end{cases} \quad (17)$$

where  $\varepsilon$  can be selected as a suitable maximum expected error of a classifier (e.g.  $\varepsilon = 0.3$ ) so that larger errors are considered as outliers by the M-estimator.

The factor  $\gamma()$  provides temporal smoothness to the measurement, by applying a running window factor with length  $\tau$  (i.e.  $\tau = 5$  frames):

$$\gamma(A_{n,t}, E_{o,t}, \tau) = \frac{1}{2\tau + 1} \sum_{i=t-\tau}^{i=t+\tau} \rho(A_{n,t}, E_{o,t}) \quad (18)$$

For the training process, we have labelled 12 video sequences 5000 frames long each (60000 labelled frames), of 3 subjects with different physiological facial attributes (and thus different eyelid amplitude values), each of them in 4 different blinking states: (awake blinking, no-blinking, long blinks, drowsy). The sequences were captured using a real vehicle (see Figure 2 for examples). The amplitude value  $A_t$  is obtained using the face alignment method in the literature (Kazemi and Sullivan, 2014).

To learn the differences between users we compute the cost maps for each subject as shown in Figure 5 (summing the cost of all sequences of each subject). As we can see the shapes of the cost map are slightly different, but showing similar minimum values (except subject 3). For an online version of the algorithm we can start with global parameters and as more values are available, we can fine tune the parameters for each user, using the proposed method.

Moreover, we have collected all the cost values spanning  $\alpha$  and  $\beta$  from 0 to 1, and as a result we have the cost map summed to all sequences is illustrated in Figure 6. The minimum cost is obtained when  $\alpha$  gets closer to 1.0, and  $\beta$  is kept behind at around 0.98. This is well aligned with the approximate values reasoned in section 3.1. However, this automatic process allows

a better fine tuning adjustment of the parameters to real driving sequences.

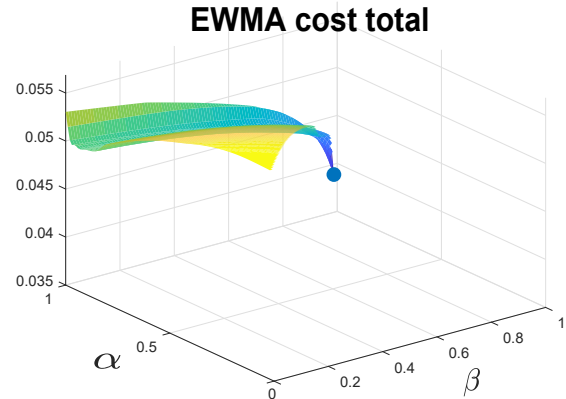


Figure 6: Map of the cost function  $J$  for  $\alpha$  and  $\beta$  values spanning from 0.0 to 1.0 in steps of 0.01.

## 4 IMPLEMENTATION

The proposed method has been implemented in C++ as part of a DMS library. This library is built as a set of modules to address specific functions, such as face detection, facial landmark tracking, face recognition, eyelid closure measurement, gaze estimation, etc. An API allows to connect complex systems with third-party libraries such as OpenCV, DLib, OpenFace, etc.

The DMS pipeline with eyelid aperture estimation was integrated into three different machines, including a standard PC (Intel i5, 8GB RAM), an embedded platform (NXP i.MX6 ARM Cortex A9, 1GB RAM), and the NVIDIA Drive PX 2 platform (2XTegra X2 SoCs). Table 1 shows the average processing time on the test sequences. As we can see, the algorithm runs in real-time for both PC and NVIDIA Drive PX 2, while still provides about 10 fps for the embedded platform, which is enough to run the application. The normalisation method consumes only a small fraction of the entire pipeline (most of the computation goes to previous stages, such as facial landmark analysis).

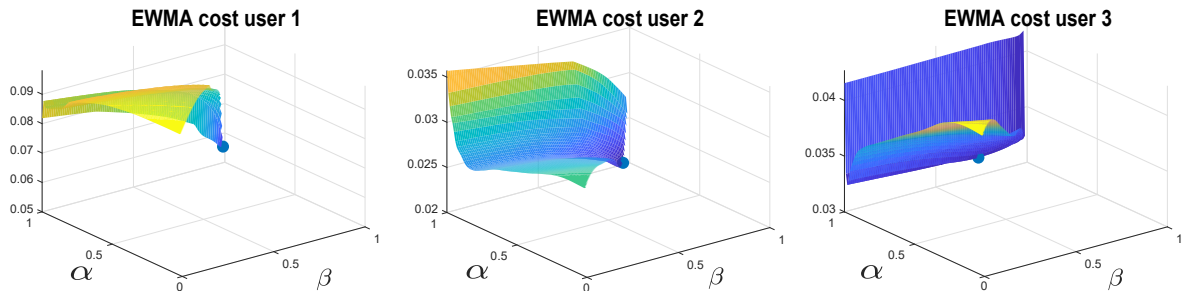


Figure 5: Map of cost function  $J$  for each user and for  $\alpha$  and  $\beta$  values spanning from 0.0 to 1.0 in steps of 0.01.

Table 1: Average computing time of the entire pipeline (including face detection and facial landmark), and the eyelid aperture estimation method alone.

	PC	Embedded	Drive PX 2
Pipeline	32.5 ms	87.7 ms	23.2 ms
Eyelid	3.1 ms	6.7 ms	2.1 ms

## 5 TESTS & DISCUSSION

To validate the benefits of normalising the eyelid amplitude, we compute the normalised eyelid aperture  $A_{n,t}$  and define a threshold of 0.8 to determine binary blink events. Since the signal is normalised for each user, the threshold is applicable to all the tested sequences and will not suffer of accuracy loss when detecting blinks (Schmidt et al., 2018). We set this value to correctly include the closing and opening phases of the blinks (i.e. eye states with eyelid aperture lower than 80% are considered as blinks).

Ground truth annotations on blink patterns in the driving context is not easily available. Therefore, to test our algorithm, we have collected sequences of three users and two arousal state with different blinking patterns (awake and drowsy). Test sequences were obtained in real driving conditions at different times of day, with volunteers inside a real car. A total of 10000 frames were captured for each user. Manual labelling of the open and blinking states was performed on the sequences.

A first evaluation of the proposed method was done using the cost function in eq. 16 and comparing it with other baseline methods. The cost function is suitable to evaluate different algorithms as it reflects the error produced with respect to a ground truth dataset. We implemented two baseline methods based on simple calculations: the envelope function and a Gaussian Mixture Model (GMM) of the eye amplitude signal  $A_t$  (eq. 2 to obtain the open,  $A_o$  and closed  $A_c$  signals; then, using eq. 1 the normalised eyelid aperture  $A_{n,t}$  is obtained. The purpose of this evaluation is to assess whether our normalisation method reduces the estimation error compared to basic signal processing alternatives.

As we can see in Table 2, the proposed method

Table 2: Cost of different methods for the 3 users and 2 blinking patterns (Normal and Drowsy). Our method (EWMA) with  $\alpha = 0.999$  and  $\beta = 0.99$  obtains the lowest average cost.

	User 1		User 2		User 3		Mean
	Normal	Drowsy	Normal	Drowsy	Normal	Drowsy	
Envelope	0.16	0.08	0.31	0.15	0.18	0.17	0.17
GMM	0.10	0.11	0.24	0.11	<b>0.03</b>	0.10	0.11
Our Method	<b>0.03</b>	<b>0.06</b>	<b>0.07</b>	<b>0.04</b>	0.06	<b>0.04</b>	<b>0.05</b>

provides the average lowest cost, and homogeneous costs for all users and type of blinking patterns. This is due to its enhanced capability to adapt to eyelid amplitude variations, which is more robust than simple metrics such as GMM or envelope computations.

A second evaluation was done based on a binary classification approach. Our aim is to compare our method's ability to correctly classify the eyes as open or closed. Therefore, we defined two eye states (classes): open and closed (blink). Accuracy values were computed for both classes (see Table 3). Other related works results are included for comparison. These methods use different evaluation datasets which were not available for our evaluation. However, our testing set share similar characteristics with their data which make our experimentation representative and comparable. In addition, further validation with common data should be done to complement the provided results.

The results in Table 3 show that the application of a user-based normalisation method before a simple threshold-based classification achieves results comparable to other more sophisticated eye state classification methods. Moreover, our method is accurate enough to classify different types of sequences of awake (normal blinks) and drowsy (microsleeps) users.

Table 3: Comparison for frame classification accuracy of open and close states. For our method  $\alpha$  and  $\beta$  with the lowest average cost was selected.

Accuracy (%)	Open	Closed	All
Sukno et al. (2009)	99.5	80.5	97.1
Qin et al. (2012)	97.0	88.7	91.6
Gou et al. (2017)	-	-	91.4
Ji et al. (2018)	96.8	96.2	97.6
Our Method (Awake)	97.3	92.1	<b>97.8</b>
Our Method (Drowsy)	99.1	95.9	<b>98.9</b>
<b>Our Method (Total)</b>	98.5	95.3	<b>98.1</b>

The results show lower accuracy for the awake sequences, specially when classifying closed (blink) eyes. These errors could be produced due to the fast transitions between open and closed eyes in normal blinks and the capturing rate of the camera ( $\approx 30fps$ ). In these situations one or two-frames error has a

greater impact on the accuracy values compared to the drowsy sequences, where blink intervals are longer. Nevertheless, the overall accuracy is higher than other results reported in related state-of-the-art methods.

Finally, the presented results suggest that including our method in more complex blink detection pipelines within Driver Monitoring Systems (DMS) improves the overall detection accuracy without adding significant computational overhead.

## 6 CONCLUSIONS

In this paper we have presented a method to obtain an eyelid aperture signal, based on online amplitude analysis, which enables driver-adaptive normalisation of eye amplitudes obtained with face alignment methods. Its parameters have been trained using manually labelled sequences and a proposed cost function with minimisation mechanisms. The method has been implemented within the framework of a Driver Monitoring System (DMS) library. Experimental results show real-time performance in different platforms used in automation applications, which make it feasible for integration in complex ADAS systems without significant computational overhead.

The method was evaluated using the proposed cost function, which makes use of manually labelled data samples. Comparison with simple baseline methods was provided showing lower error cost. In addition, the results of the classification problem for open and closed eyes show higher accuracy and adaptability to driver-specific visual features compared to other state-of-the-art methods.

Our method can be incorporated into blink detection pipelines to improve the estimation of blink parameters while it also produces adaptive eyelid aperture estimates valuable for subsequent driver's arousal state analysis. Future work include the validation of the method under a wide variety of use cases and conditions, extending our current database.

## ACKNOWLEDGEMENTS

This work has received funding from the European Union's H2020 research and innovation programme (grant agreement n° 690772, project VI-DAS).

## REFERENCES

Asthana, A., Zafeiriou, S., Cheng, S., and Pantic, M. (2014). Incremental face alignment in the wild. *IEEE*

*Conference on Computer Vision and Pattern Recognition, CVPR*, pages 1859–1866.

Baccour, M. H., Driewer, F., Kasneci, E., and Rosenstiel, W. (2019). Camera-Based Eye Blink Detection Algorithm for Assessing Driver Drowsiness. In *IEEE Intelligent Vehicles Symposium*, pages 866–872.

Baltrusaitis, T., Robinson, P., and Morency, L. P. (2016). OpenFace: An open source facial behavior analysis toolkit. In *2016 IEEE Winter Conference on Applications of Computer Vision, WACV 2016*.

Borghini, G., Astolfi, L., Vecchiato, G., Mattia, D., and Babiloni, F. (2014). Measuring neurophysiological signals in aircraft pilots and car drivers for the assessment of mental workload, fatigue and drowsiness. *Neuroscience and Biobehavioral Reviews*, 44:58–75.

Boyle, L. N., Tippin, J., Paul, A., and Rizzo, M. (2008). Driver performance in the moments surrounding a microsleep. *Transportation Research Part F: Traffic Psychology and Behaviour*, 11(2):126–136.

Cabrall, C., Janssen, N., Goncalves, J., Morando, A., Sassman, M., and de Winter, J. (2016). Eye-based driver state monitor of distraction, drowsiness, and cognitive load for transitions of control in automated driving. *2016 IEEE International Conference on Systems, Man, and Cybernetics (SMC)*, pages 001981–001982.

Daniluk, M., Rezaei, M., Nicolescu, R., and Klette, R. (2014). Eye Status Based on Eyelid Detection : A Driver Assistance System. In *International Conference on Computer Vision and Graphics*.

Danisman, T., Bilasco, I. M., Djeraba, C., and Ihaddadene, N. (2010). Drowsy driver detection system using eye blink patterns. In *International Conference on Machine and Web Intelligence, ICMWI*, pages 230–233.

Drutarovsky, T. and Fogelton, A. (2015). Eye blink detection using variance of motion vectors. In *Proceedings of 2th workshop on Assistive Computer Vision and Robotics in ECCV 2014*, volume 8927.

Ebrahim, P., Stolzmann, W., and Yang, B. (2013). Eye movement detection for assessing driver drowsiness by electrooculography. *Proceedings - 2013 IEEE International Conference on Systems, Man, and Cybernetics, SMC 2013*, pages 4142–4148.

European Commission (2011). Roadmap to a Single European Transport Area—Towards a competitive and resource efficient transport system. Technical report, European Commission.

Fogelton, A. and Benesova, W. (2016). Eye blink detection based on motion vectors analysis. *Computer Vision and Image Understanding*, 148:23–33.

Fridman, L., Lee, J., Reimer, B., and Victor, T. (2016). Owl and Lizard: Patterns of Head Pose and Eye Pose in Driver Gaze Classification. *IET Computer Vision*, 10(4):1–9.

Friedrichs, F. and Yang, B. (2010). Camera-based drowsiness reference for driver state classification under real driving conditions. In *IEEE Intelligent Vehicles Symposium*, volume 4, pages 101–106.

Fuhl, W., Santini, T., and Kasneci, E. (2017). Fast & robust eyelid outline & aperture detection in real-world sce-

- narios. In *IEEE Winter Conference on Applications of Computer Vision*.
- García, I., Bronte, S., Bergasa, L. M., Almazán, J., and Yebes, J. (2012). Vision-based drowsiness detector for real driving conditions. In *IEEE Intelligent Vehicles Symposium, Proceedings*, pages 618–623.
- Goenettea, J., Unzueta, L., Elordi, U., Ortega, J. D., and Otaegui, O. (2018). Efficient monocular point-of-gaze estimation on multiple screens and 3D face tracking for driver behaviour analysis. In *6th Int. Conf. on Driver Distraction and Inattention*, pages 1–8.
- González-Ortega, D., Díaz-Pernas, F. J., Antón-Rodríguez, M., Martínez-Zarzuela, M., and Díez-Higuera, J. F. (2013). Real-time vision-based eye state detection for driver alertness monitoring. *Pattern Analysis and Applications*, 16(3):285–306.
- Gou, C., Wu, Y., Wang, K., Wang, K., Wang, F. Y., and Ji, Q. (2017). A joint cascaded framework for simultaneous eye detection and eye state estimation. *Pattern Recognition*, 67:23–31.
- Han, W., Yang, Y., Huang, G. B., Sourina, O., Klanner, F., and Denk, C. (2016). Driver Drowsiness Detection Based on Novel Eye Openness Recognition Method and Unsupervised Feature Learning. In *IEEE International Conference on Systems, Man, and Cybernetics, SMC*, pages 1470–1475.
- Ji, Y., Wang, S., Lu, Y., Wei, J., and Zhao, Y. (2018). Eye and mouth state detection algorithm based on contour feature extraction. *Journal of Electronic Imaging*, 27(05):1.
- Kaplan, S., Guvensan, M. A., Yavuz, A. G., and Karalurt, Y. (2015). Driver Behavior Analysis for Safe Driving: A Survey. *IEEE Transactions on Intelligent Transportation Systems*, 16(6):3017–3032.
- Kazemi, V. and Sullivan, J. (2014). One millisecond face alignment with an ensemble of regression trees. *Proceedings of the IEEE Computer Society Conference on Computer Vision and Pattern Recognition*, pages 1867–1874.
- King, D. E. (2009). Dlib-ml: A Machine Learning Toolkit. *Journal of Machine Learning Research*, 10:1755–1758.
- Mandal, B., Li, L., Wang, G. S., and Lin, J. (2017). Towards Detection of Bus Driver Fatigue Based on Robust Visual Analysis of Eye State. *IEEE Transactions on Intelligent Transportation Systems*, 18(3):545–557.
- Nopsuwanchai, R., Noguchi, Y., Ohsuga, M., Kamakura, Y., and Inoue, Y. (2008). Driver-independent assessment of arousal states from video sequences based on the classification of eyeblink patterns. In *IEEE Conference on Intelligent Transportation Systems, Proceedings, ITSC*, pages 917–924.
- Qin, H., Liu, J., and Hong, T. (2012). An eye state identification method based on the embedded hidden Markov model. *IEEE International Conference on Vehicular Electronics and Safety, ICVES*, pages 255–260.
- SAE International (2018). Taxonomy and Definitions for Terms Related to Driving Automation Systems for On-Road Motor Vehicles. Technical report, SAE International.
- SafetyNet (2009). Fatigue. Technical report, European Commission Project.
- Schmidt, J., Laarousi, R., Stolzmann, W., and Karrer-Gauß, K. (2018). Eye blink detection for different driver states in conditionally automated driving and manual driving using EOG and a driver camera. *Behavior Research Methods*, 50(3):1088–1101.
- Sikander, G. and Anwar, S. (2019). Driver Fatigue Detection Systems: A Review. *IEEE Transactions on Intelligent Transportation Systems*, 20(6):2339–2352.
- Soukupová, T. and Cech, J. (2016). Real-Time Eye Blink Detection using Facial Landmarks. In *21st Computer Vision Winter Workshop*.
- Sukno, F. M., Pavani, S. K., Butakoff, C., and Frangi, A. F. (2009). Automatic assessment of eye blinking patterns through statistical shape models. In *International Conference on Computer Vision Systems, ICVS*, volume 5815 LNCS, pages 33–42.
- Wang, L., Ding, X., Fang, C., Liu, C., and Wang, K. (2009). Eye blink detection based on eye contour extraction. In *Proceedings of SPIE - The International Society for Optical Engineering*, volume 7245.
- Yang, F., Yu, X., Huang, J., Yang, P., and Metaxas, D. (2012). Robust eyelid tracking for fatigue detection. In IEEE, editor, *19th IEEE International Conference on Image Processing (ICIP)*, pages 1829–1832.